

Photophysical aspects of C–H bond activation in rhodium dicarbonyl complexes

Agus A. Purwoko, Denis P. Drolet, Alistair J. Lees *

Department of Chemistry, Binghamton University State, University of New York at Binghamton, Binghamton, NY 13902-6016, USA

Received 5 January 1995; in revised form 6 April 1995

Abstract

The solution photochemistry of C–H bond activating $\text{CpRh}(\text{CO})_2$, $\text{Cp}^*\text{Rh}(\text{CO})_2$ and $(\text{HBPz}_3^*)\text{Rh}(\text{CO})_2$ complexes ($\text{Cp} = \eta^5\text{-C}_5\text{H}_5$; $\text{Cp}^* = \eta^5\text{-C}_5\text{Me}_5$; $\text{HBPz}_3^* = \text{tris}(3,5\text{-dimethylpyrazolyl})\text{borate}$) has been investigated at several excitation wavelengths. Quantitative photochemical measurements have been obtained for ligand photosubstitution and intermolecular Si–H/C–H bond activation reactions through a determination of absolute quantum efficiencies. In each complex the results reveal that the photochemistry is extremely wavelength dependent and two low lying ligand field (LF) excited states are implicated in the mechanism. Population of the upper energy LF excited state leads to effective CO dissociation and subsequent Si–H/C–H bond activation, whereas excitation into the lower energy LF excited state results in inefficient photochemistry. These experimental observations are related to the electronic absorption characteristics of the molecules and are interpreted on a photophysical scheme involving excited states with quite distinct photochemical reactivities.

Keywords: Rhodium; Photochemistry; C–H bond activation

1. Introduction

Considerable attention has been paid in recent years to studying the special reactivity of C–H bond activating systems and the ability of transition-metal complexes to insert into saturated carbon centers under relatively mild homogeneous conditions [1]. Among organometallic systems there has been much interest in the photochemistry of CpML_2 and Cp^*ML_2 ($\text{Cp} = \eta^5\text{-C}_5\text{H}_5$; $\text{Cp}^* = \eta^5\text{-C}_5\text{Me}_5$; $\text{M} = \text{Rh, Ir}$; $\text{L} = \text{CO, C}_2\text{H}_4, \text{PR}_3$) as these complexes yield oxidative addition products from the intermolecular C–H bond activation of hydrocarbon bonds upon light irradiation [2,3]. Recently, the photochemically-induced C–H activation of the analogous $(\text{HBPz}_3^*)\text{Rh}(\text{CO})_2$ ($\text{Pz}_3^* = 3,5\text{-dimethylpyrazolyl}$) complex has also been reported [4].

Several experimental approaches have been taken in an effort to learn about the photochemical reactivity in these types of molecules and to characterize the primary photoproducts and other key reaction intermediates in-

involved in the mechanism. For instance, in the case of the above cyclopentadienyl rhodium and iridium complexes steady-state photolyses [5], time-resolved spectroscopic techniques [6], matrix isolation studies [7], gas phase experiments [8], and low-temperature measurements in liquefied noble gas solvents [9] have all been employed in efforts to identify the reaction intermediates. The results clearly establish that the $\text{CpM}(\text{CO})$ and $\text{Cp}^*\text{M}(\text{CO})$ ($\text{M} = \text{Rh, Ir}$) monocarbonyl complexes, which are formally $16e^-$ species, are initially produced and are responsible for the intermolecular C–H bond activation, although it should be recognized that these intermediates are extremely short-lived and not observed directly in solution. Indeed, under such conditions these monocarbonyl complexes are only detected spectroscopically as solvated adducts, $\text{CpM}(\text{CO}) \cdots \text{S}$ and $\text{Cp}^*\text{M}(\text{CO}) \cdots \text{S}$ ($\text{S} = \text{solvent molecule, such as alkane or liquefied noble gas}$), before undergoing rapid C–H activation [4–8]. Similarly, in recent studies of the solution photochemistry of $(\text{HBPz}_3^*)\text{Rh}(\text{CO})_2$ ($\text{HBPz}_3^* = \text{tris}(3,5\text{-dimethylpyrazolyl})\text{borate}$) it has been suggested that the mechanism of this efficient C–H bond activator also involves rapid CO dissociation from the metal center [10].

* Corresponding author.

Despite the better understanding reached concerning the intermediates in these photochemically-induced C–H activation reactions, it is apparent that much less is known about the influence of the molecule's photophysical pathways. These initial photochemical events are significant because it is these routes that lead to the primary photoproducts and ultimately influence the reaction mechanism for C–H activation and its efficiency. In this paper we provide additional data pertaining to the solution photochemistry of the C–H bond activating $\text{CpRh}(\text{CO})_2$, $\text{Cp}^*\text{Rh}(\text{CO})_2$ and $(\text{HBPz}_3^*)\text{Rh}(\text{CO})_2$ systems following our earlier reports [5,10]. In particular we are now able to draw attention to a number of common photophysical features that exist in these highly reactive molecules.

2. Experimental

2.1. Syntheses

The $\text{CpM}(\text{CO})_2$ ($M = \text{Rh}, \text{Ir}$) complexes were prepared according to literature methods [12], except for $\text{Cp}^*\text{Rh}(\text{CO})_2$, which was purchased from Strem Chemicals. IR, $\text{CpRh}(\text{CO})_2$ in decalin: $\nu(\text{CO})$ 2046, 1982 cm^{-1} (lit. [12a] as a liquid, 2051, 1987 cm^{-1}). The $(\text{HBPz}_3^*)\text{Rh}(\text{CO})_2$ complex was prepared via reaction of chlorodicarbonylrhodium(I) dimer with potassium hydrotris(3,5-dimethylpyrazolyl)borate according to a procedure described by Ghosh [4b]. IR, $(\text{HBPz}_3^*)\text{Rh}(\text{CO})_2$ in *n*-pentane: $\nu(\text{CO})$ 2054, 1980 cm^{-1} (lit. [4b] in *n*-hexane, 2054, 1981 cm^{-1}).

2.2. Equipment and procedures

UV-visible and FTIR spectra were recorded on Hewlett-Packard Model 8450A diode-array and Nicolet Model 20SXC spectrometers, respectively. Emission spectra were recorded on a SLM Instruments Model 8000/8000S dual monochromator spectrometer, which incorporates a red-sensitive Hamamatsu R928 photomultiplier tube and photon-counting facilities. Samples were maintained at 77 K as solids or EPA glassy solutions with an Oxford Instruments DN1704K variable temperature liquid- N_2 -cooled cryostat fitted with synthetic sapphire inner windows and quartz outer windows.

In all photolysis experiments the solution temperatures were controlled to ± 0.1 K between 268 and 293 K by circulating a thermostatted ethylene glycol + water mixture through a jacketed cell holder. Solutions were stringently filtered through 0.22 μm Millipore filters and deoxygenated by purging with prepurified nitrogen gas for 15 min prior to irradiation. Solutions saturated with CO were obtained by initially bubbling CO gas through the solution for 30 min and then stirring the

solution for a further 30 min under a sealed CO atmosphere. During photolysis the solutions were rapidly stirred to ensure sample homogeneity and a uniform optical density in the light path. UV-visible and FTIR spectra were obtained from solutions at regular intervals throughout irradiation; resultant quantum efficiency values were determined in triplicate and were found to be reproducible to within $\pm 5\%$ in all cases. The photochemical substitution measurements involving the phosphine and phosphite ligands were performed at 268 K to minimize the effects of competing thermal reactions. Ligand substitution reactions were also measured in the dark to assess the extent of thermal processes and the reported quantum efficiency values are corrected for this contribution (typically 4–8% under our experimental conditions).

A Lexel Corp. Model 95-4 4 W argon-ion laser was used to perform the visible photolyses at 458 nm; the incident laser light intensity was calibrated by means of a Lexel Corp. Model 504 external power meter. Typically laser powers of 100–200 mW ($2.3\text{--}4.6 \times 10^{-5}$ einstein min^{-1}) were employed for irradiation of $\text{CpRh}(\text{CO})_2$, although results were also obtained with reduced laser light powers of between 30 and 75 mW and the determined quantum efficiency values were not changed. For the 458 nm excitations of $(\text{HBPz}_3^*)\text{Rh}(\text{CO})_2$ the typical incident laser power used was 20 mW (4.6×10^{-6} einstein min^{-1}). Samples were irradiated with UV light from an Ealing Corp. medium-pressure 200 W mercury arc lamp and housing apparatus set on an optical rail, and 10 nm bandpass interference filters (Ealing Corp.) were used to isolate the excitation wavelength. The incident light intensities were determined by ferrioxalate and Aberchrome 540 actinometry [13], and were typically in the range of $5.2\text{--}11.3 \times 10^{-7}$ einstein min^{-1} .

3. Results and discussion

3.1. Electronic absorption spectra

UV-visible data were recorded for the $\text{CpM}(\text{CO})_2$, $\text{Cp}^*\text{M}(\text{CO})_2$ and $(\text{HBPz}_3^*)\text{Rh}(\text{CO})_2$ complexes in room-temperature alkane solvent (see Table 1). In each

Table 1
Lowest lying electronic absorption bands of $\text{CpM}(\text{CO})_2$, $\text{Cp}^*\text{M}(\text{CO})_2$ and $(\text{HBPz}_3^*)\text{Rh}(\text{CO})_2$ complexes in decalin at 298 K

Complex	λ_{max} (nm)	ϵ ($\text{M}^{-1} \text{cm}^{-1}$)
$\text{CpRh}(\text{CO})_2$	425 (sh)	78
$\text{Cp}^*\text{Rh}(\text{CO})_2$	505	152
$\text{CpIr}(\text{CO})_2$	355 (sh)	144
$\text{Cp}^*\text{Ir}(\text{CO})_2$	380 (sh)	67
$(\text{HBPz}_3^*)\text{Rh}(\text{CO})_2$ ^a	356	2100

^a Recorded in *n*-pentane.

case the lowest lying electronic transition appears as a weak band (or a shoulder) in the near-UV or visible regions; the lowest energy absorption band of (HBPz₃^{*})Rh(CO)₂ is significantly more intense. These lowest lying absorptions are believed to be ligand field (LF) transitions because the molar absorptivities are so low and their energy positions are consistent with the ligand field strengths of these d⁸ metals (the analogous CpCo(CO)₂ complex is red) [14]. Furthermore, the energy position of each of these lowest energy absorption bands shows relatively little solvent dependence, in accordance with the LF assignment [14,15].

While these lowest lying transitions are of particular significance with respect to the photochemistry, higher energy absorption bands are also observed for each of these complexes in the UV region: e.g., CpRh(CO)₂ in decalin, 286 nm ($\epsilon = 3820 \text{ M}^{-1} \text{ cm}^{-1}$) [5c], Cp^{*}Ir(CO)₂ in *n*-hexane, 220 nm ($\epsilon = 13000 \text{ M}^{-1} \text{ cm}^{-1}$) [4a] and (HBPz₃^{*})Rh(CO)₂ in *n*-hexane, 221 nm ($\epsilon = 17600 \text{ M}^{-1} \text{ cm}^{-1}$) [4a]. In the latter two complexes these transitions are comparatively much more intense than their lowest energy features and almost certainly reflect charge transfer characteristics [14,15].

Finally, it should be noted that the extremely low molar absorptivity of the lowest energy bands in the Cp and Cp^{*} complexes (see Table 1) implies that these transitions may have considerably more triplet character. In contrast, the more intense lowest lying absorption of (HBPz₃^{*})Rh(CO)₂ is consistent with a singlet (¹LF) band, suggesting that the corresponding triplet feature is unresolved (this point is further discussed below). Indeed, most ³LF bands of organometallic complexes are too weak to be observed directly and are usually buried under overlapping charge transfer absorptions [14], but a few examples where they have been identified are W(CO)₅(pip) (pip = piperidine), ¹LF is at 407 nm ($\epsilon = 3960 \text{ M}^{-1} \text{ cm}^{-1}$) and ³LF is at 443 nm ($\epsilon = 560 \text{ M}^{-1} \text{ cm}^{-1}$) [16], and W(CO)₄en (en = ethylenediamine), ¹LF is at 397 nm ($\epsilon = 1400 \text{ M}^{-1} \text{ cm}^{-1}$) and ³LF is at 450 nm ($\epsilon = 400 \text{ M}^{-1} \text{ cm}^{-1}$) [17]. It ought to be stated, however, that the use of the spin multiplicity terms ‘singlet’ and ‘triplet’ for these heavy-atom excited states is not strictly appropriate because of the large extent of spin-orbit coupling in these molecules [18]. Consequently, these excited states should be regarded as being heavily mixed in terms of their spin designations.

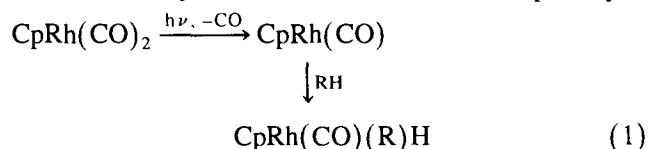
3.2. Luminescence observations

Emission measurements were carried out at 77 K from CpRh(CO)₂, Cp^{*}Rh(CO)₂ and (HBPz₃^{*})Rh(CO)₂ in EPA glassy solutions and as solids. Spectra were recorded between 350 and 700 nm on a photon-counting luminescence spectrophotometer and no luminescence features were observed from any of the complexes following excitation into their lowest energy absorption

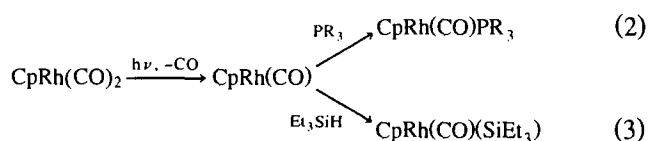
bands. This result is concordant with extremely rapid nonradiative decay from the lowest energy excited states in these molecules and hence the LF assignments [18].

3.3. Photochemical reactivity

The solution photochemistry of CpRh(CO)₂ and Cp^{*}Rh(CO)₂ has recently been investigated in considerable detail [5b,c] and the C–H bond activation reaction is understood to take place via an initial CO dissociation step (Eq. (1)). However, the photoproduct is found to be unstable over the period of light irradiation. Previously it has been shown in flash photolysis



measurements that CpRh(CO)(R)H undergoes reductive elimination ($k > 3 \times 10^3 \text{ s}^{-1}$) to form bridged [CpRh(μ -CO)]₂, and subsequently more slowly to Cp₂Rh₂(CO)₃ [6b]. As noted above, the CpRh(CO) monocarbonyl complex is highly unstable and rapidly forms a solvent adduct, CpRh(CO) ··· S, before yielding photoproduct [5–9]. Consequently, in order to study the photochemistry quantitatively an entering ligand must be added in excess concentration; we have chosen to use phosphine and phosphite (PR₃) nucleophiles, or triethylsilane (Et₃SiH), each of which is known to effectively scavenge the monocarbonyl intermediate (see Eqs. (2) and (3)) [5c].



UV-visible absorption spectral changes observed accompanying the 313 nm photolysis of $2.5 \times 10^{-3} \text{ M}$ CpRh(CO)₂ in decalin containing 0.05 M P(ⁿBu)₃ at 268 K are depicted in Fig. 1. During the course of the light excitation these spectra reveal a slight absorption increase. The data were recorded at 10 min irradiation time intervals and are typical of those observed for the ligand photosubstitution reaction (Eq. (2)). FTIR spectra were simultaneously obtained and they indicate a decline of the reactant's $\nu(\text{CO})$ bands centered at 2046 and 1982 cm⁻¹ with a concurrent increase of a new $\nu(\text{CO})$ feature at 1940 cm⁻¹, representative of the monocarbonyl CpRh(CO)P(ⁿBu)₃ photoproduct (lit. [5c] in *n*-pentane, 1943 cm⁻¹). These FTIR spectra are also analogous to those observed for this ligand photosubstitution reaction as described previously [5c]. Importantly, the observed spectral changes illustrate that there is a smooth conversion of reactant to product in a photochemical process that is uncomplicated by side or subsequent reactions.

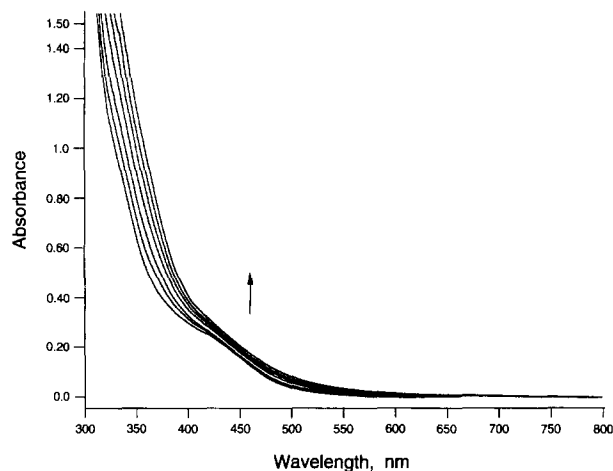
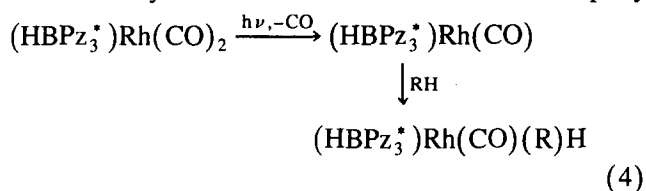


Fig. 1. UV-visible absorption spectra accompanying the 313 nm photolysis of 2.5×10^{-3} M $\text{CpRh}(\text{CO})_2$ in deoxygenated decalin containing 0.05 M $\text{P}(\text{n-Bu})_3$ at 268 K. Initial spectrum was observed prior to irradiation; subsequent spectra were recorded following 10 min time intervals.

For $(\text{HBPz}_3^*)\text{Rh}(\text{CO})_2$ it is determined that the light-induced C–H bond activation (Eq. (4)) can be directly monitored spectroscopically without any interference in the photochemical transformation [10]. Again, the photochemistry is understood to proceed via a monocarbonyl intermediate which is solvated rapidly



after the initial CO extrusion; however, in this case it is found that the photoproduct is stable in solution.

UV-visible absorption spectral changes accompanying the 366 nm photolysis of 3.5×10^{-3} M $(\text{HBPz}_3^*)\text{Rh}(\text{CO})_2$ in *n*-heptane at 293 K are shown in Fig. 2.

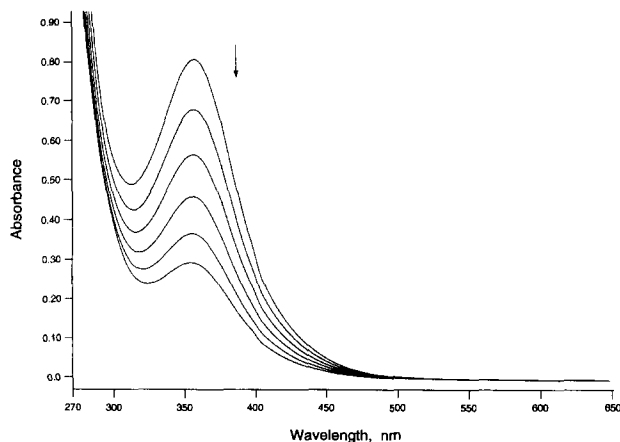


Fig. 2. UV-visible absorption spectra accompanying the 366 nm photolysis of 3.5×10^{-3} M $(\text{HBPz}_3^*)\text{Rh}(\text{CO})_2$ in deoxygenated *n*-heptane at 293 K. Initial spectrum was observed prior to irradiation; subsequent spectra were recorded following 45 s time intervals.

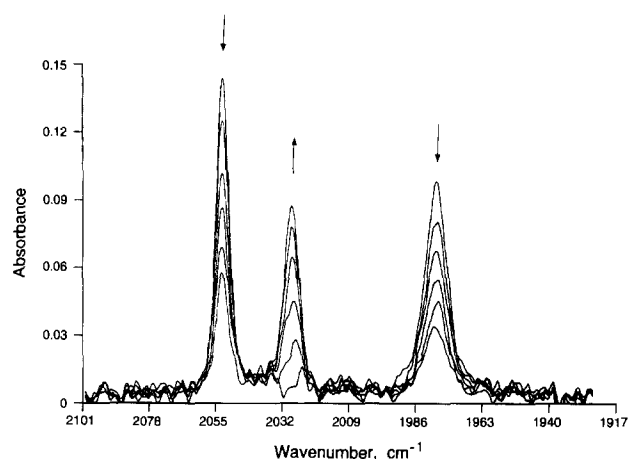


Fig. 3. FTIR absorption spectra accompanying the 366 nm photolysis of 3.5×10^{-3} M $(\text{HBPz}_3^*)\text{Rh}(\text{CO})_2$ in deoxygenated *n*-heptane at 293 K. Initial spectrum was observed prior to irradiation; subsequent spectra were recorded following 45 s time intervals.

These spectra were obtained at 45 s irradiation time intervals and are representative of the intermolecular C–H bond activation reaction in hydrocarbon media [4,10b]. Throughout this reaction the spectra display a decreasing absorption. FTIR spectra were recorded simultaneously during this C–H bond activation process and are shown in Fig. 3; these illustrate a decline in the reactant's $\nu(\text{CO})$ bands centered at 2054 and 1980 cm^{-1} , with a concurrent growth of a new $\nu(\text{CO})$ feature at 2028 cm^{-1} representing the monocarbonyl hydrido $(\text{HBPz}_3^*)\text{Rh}(\text{CO})(\text{C}_7\text{H}_{15})\text{H}$ product [4,10b,19]. The photochemistry here is once again clean and complete conversion can be achieved to the oxidative addition product without interference from secondary photoreactions [10b].

3.4. Photochemical quantum efficiencies

Absolute quantum efficiencies (ϕ_{cr}) have been obtained at several different excitation wavelengths for the above photosubstitution and Si–H/C–H activation processes (Eqs. (2)–(4)). The ϕ_{cr} values were in each case determined by monitoring the decline of the reactant's electronic absorption and infrared $\nu(\text{CO})$ bands (over at least 80% of reaction) and application of Eq. (5).

$$-dC_{\text{R}}/dt = \phi_{\text{cr}} I_0 (1 - 10^{-D}) \epsilon_{\text{R}} b C_{\text{R}} / D \quad (5)$$

Here, C_{R} is the concentration of the reactant complex at varying photolysis times t , I_0 is the incident light intensity per unit solution volume, b is the cell path-length, and D and ϵ_{R} are the optical density of the solution and molar absorptivity of the reactant complex at the irradiation wavelength, respectively. It should be noted that D is the total optical density of the solution and represents both of the absorbing species; the factor $\epsilon_{\text{R}} b C_{\text{R}} / D$ is the fraction of the absorbed light that is absorbed by the reactant complex in the solution mix-

ture. Plots of $\ln[(A_t - A_\infty)/(A_0 - A_\infty)]$ versus $\int_0^t [(1 - 10^{-D})/D] dt$, where A_0 , A_t and A_∞ are the infrared absorbance values of the reactant's $\nu(\text{CO})$ bands throughout photolysis, were observed to yield straight lines of slope α to reaction completion, with $\alpha = -\phi_{\text{cr}} I_0 \epsilon_R b$. The plots revealed linearity when $A_\infty = 0$ and yielded coincident α values following kinetic analysis at either of the reactant's $\nu(\text{CO})$ bands. Additionally, α results obtained in each case on monitoring the increasing $\nu(\text{CO})$ absorbance of the photoproduct give the same value. These kinetic observations confirm the stoichiometric nature of the photochemical conversions.

Under the photochemical reaction conditions employed the obtained ϕ_{cr} values represent the efficiency of dissociation from the excited states to form the monocarbonyl intermediate [5c,10b]. Subsequently, this species is scavenged by the excess ligand to form the photoproduct quantitatively. Quantum efficiencies for Si–H bond activation were recorded on photolysis of the $\text{CpRh}(\text{CO})_2$ and $\text{Cp}^*\text{Rh}(\text{CO})_2$ complexes with varying concentrations of Et_3SiH (see Table 2). The results illustrate that there is a negligible dependence on Et_3SiH concentration and are entirely consistent with a dissociative mechanism involving CO extrusion as the initial photochemical step and then rapid reaction with the excess concentration of scavenging ligand, as discussed previously [5c]. Lower values of ϕ_{cr} are noted for $\text{Cp}^*\text{Rh}(\text{CO})_2$; this observation has been discussed previously and is believed to be a consequence of the increased number of nonradiative relaxation pathways in the Cp^* ligand [5c].

The effects of changing the excitation wavelength are also shown in Table 2, which reports the efficiency of Si–H bond activation following irradiation of $\text{CpRh}(\text{CO})_2$ at two different wavelengths. The results

Table 2

Absolute photochemical quantum efficiencies (ϕ_{cr}) for the intermolecular Si–H bond activation reaction of $\text{CpRh}(\text{CO})_2$ and $\text{Cp}^*\text{Rh}(\text{CO})_2$ in decalin at 293 K

Complex	Excitation wavelength (nm)	Et_3SiH concentration (M)	ϕ_{cr}^a
$\text{CpRh}(\text{CO})_2$	313	0.05	0.15
		0.10	0.17
		0.20	0.19
		0.30	0.20
	458	0.05	0.0023
		0.10	0.0024
		0.20	0.0026
		0.30	0.0025
$\text{Cp}^*\text{Rh}(\text{CO})_2$	458	0.05	0.00010
		0.10	0.00011
		0.20	0.00013
		0.30	0.00012

^a Values were determined in triplicate and found to be reproducible to $\pm 5\%$.

Table 3

Absolute photochemical quantum efficiencies (ϕ_{cr}) for the photosubstitution and intermolecular C–H bond activation reactions of $\text{CpRh}(\text{CO})_2$ in decalin at 268 K and $(\text{HBPz}_3^*)\text{Rh}(\text{CO})_2$ in *n*-heptane and *n*-pentane at 293 K

Complex	Entering ligand ^a	Excitation wavelength (nm)	ϕ_{cr}^b
$\text{CpRh}(\text{CO})_2$	PMe_3	313	0.25
		458	0.0052
	PEt_3	313	0.18
		458	0.0043
	P^nBu_3	313	0.22
		458	0.0031
	$\text{P}(\text{O}-\text{Me})_3$	313	0.17
		458	0.0040
	$\text{P}(\text{O}-^n\text{Bu})_3$	313	0.16
458		0.0060	
$(\text{HBPz}_3^*)\text{Rh}(\text{CO})_2$	C_7H_{16}	366	0.31
		458	0.010
	C_5H_{12}	313	0.34
		366	0.32
		405	0.15
		458	0.011

^a Phosphine and phosphite concentrations were 0.05 M for each reaction; the hydrocarbons C_5H_{12} and C_7H_{16} were neat solvents at 8.7 and 6.8 M, respectively.

^b Values were determined in triplicate and found to be reproducible to $\pm 5\%$.

clearly demonstrate that excitation at 313 nm leads to substantially higher ϕ_{cr} values than excitation at 458 nm. This unequivocally demonstrates that the higher energy excited state of $\text{CpRh}(\text{CO})_2$ is able to undergo much more facile CO dissociation than the lower energy excited state, which is almost unreactive. Similar conclusions can be drawn on the basis of the quantum efficiencies for ligand photosubstitution of $\text{CpRh}(\text{CO})_2$ and the intermolecular C–H bond activation reaction of $(\text{HBPz}_3^*)\text{Rh}(\text{CO})_2$ (see Table 3). In each case UV excitations (313–366 nm) are much more effective at forming photoproducts than visible irradiations (405–458 nm).

As noted above, the upper energy LF excited state is understood to react rapidly to form a monocarbonyl intermediate; indeed, CO extrusions following UV excitation are commonly observed from metal carbonyl complexes [14,18]. In sharp contrast, however, the lower energy LF state in each of the $\text{CpRh}(\text{CO})_2$ and $(\text{HBPz}_3^*)\text{Rh}(\text{CO})_2$ complexes is apparently unable to effectively form photoproduct. This latter finding is consistent with previous observations and it has been suggested that a ligand rearrangement mechanism occurs from the lowest excited states in each of these complexes. For $\text{CpRh}(\text{CO})_2$ and $\text{Cp}^*\text{Rh}(\text{CO})_2$ the cyclopentadienyl ring is postulated to undergo an effective ring slippage ($\eta^5\text{-}\eta^3$) mechanism [5c], whereas in $(\text{HBPz}_3^*)\text{Rh}(\text{CO})_2$ a facile ligand dechelation ($\eta^3\text{-}\eta^2$) process has been invoked [10b]. Such mechanisms

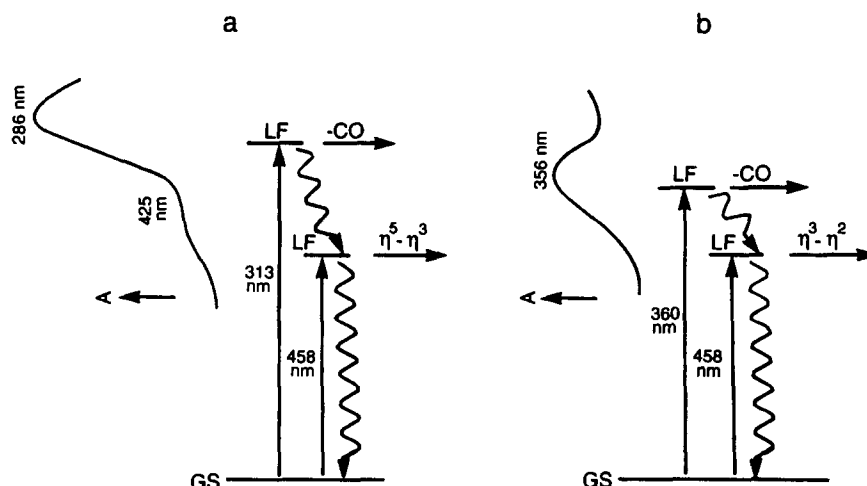


Fig. 4. Photophysical description of the lowest-lying energy levels of (a) $\text{CpRh}(\text{CO})_2$ and (b) $(\text{HBPz}_3^*)\text{Rh}(\text{CO})_2$ complexes.

clearly influence the quantum efficiencies but are inconsequential with respect to the overall photochemistry, as these ligand rearrangement reactions return the intermediates to starting materials. It should also be noted that quantum efficiencies at any of the excitation wavelengths were found to be unaffected when the solutions were previously saturated with CO gas (ca. 9×10^{-3} M). This result is consistent with an extremely rapid and quantitative reaction of the photoproducted monocarbonyl complex with scavenging ligands or the hydrocarbon substrate.

In summary, the ϕ_{cr} data obtained clearly portray that the photophysical and photochemical properties of the upper LF excited state are quite distinct from those of the lower LF excited level (see Fig. 4). In the case of $\text{CpRh}(\text{CO})_2$ excitation into the weak ^3LF absorption band at 425 nm results in inefficient photosubstitution and Si–H bond activation reactions [$\phi_{\text{cr}}(458) = 0.0023\text{--}0.006$], whereas irradiation into the upper LF absorption band at 286 nm leads to efficient photochemistry [$\phi_{\text{cr}}(313) = 0.15\text{--}0.25$]. Similar photophysical characteristics are also observed for $(\text{HBPz}_3^*)\text{Rh}(\text{CO})_2$, with inefficient C–H bond activation taking place on photolysis into the tail of the absorption envelope that comprises the lower LF state [$\phi_{\text{cr}}(458) = 0.01$], whereas excitation into the upper LF absorption band at 356 nm results in effective photochemistry [$\phi_{\text{cr}}(366) = 0.32$]. Obviously, the lowest energy LF excited states in each of the $\text{CpRh}(\text{CO})_2$ and $(\text{HBPz}_3^*)\text{Rh}(\text{CO})_2$ complexes are behaving very differently from both a quantitative and a qualitative photochemical viewpoint. In either case, the LF excitation will result in the population of higher lying σ^* orbitals, leading to rapid cleavage of M–CO, M–Cp and M–Pz * bonds. Different metal $d\sigma^*$ orbitals are apparently produced because the photochemical reactivities are so divergent. These and other photophysical aspects of these C–H

bond activating molecules are currently being further investigated.

4. Conclusions

The solution photochemistry of $\text{CpRh}(\text{CO})_2$, $\text{Cp}^*\text{Rh}(\text{CO})_2$ and $(\text{HBPz}_3^*)\text{Rh}(\text{CO})_2$ has been investigated both qualitatively and quantitatively at several excitation wavelengths and several parallel observations have been made. In each complex there is a strong wavelength-dependent photochemistry and two highly reactive LF electronically excited states are invoked to explain the ligand photosubstitution and intermolecular Si–H/C–H bond activation processes. The lower energy excited LF state is populated on visible excitation (458 nm) and is virtually unreactive towards Si–H/C–H bonds; reaction intermediates are implicated that originate from ligand rearrangements involving ring slippage and dechelation mechanisms. Contrastingly, the upper energy excited LF level is populated on UV excitation (313–366 nm) and is highly reactive in hydrocarbon solvents; it is implied that the primary photoproducts are monocarbonyl complexes which are able to undergo efficient intermolecular Si–H and C–H bond activation processes.

Acknowledgements

We are grateful to the Division of Chemical Sciences, Office of Basic Energy Sciences, Office of Energy Research, U.S. Department of Energy (Grant DE-FG02-89ER14039) for support of this research and to the Ministry of Education of the Republic of Indonesia for a graduate fellowship to A.A.P. We also thank

Professor W.A.G. Graham (University of Alberta) for initially providing a sample of $(\text{HBPz}_3^+)_2\text{Rh}(\text{CO})_2$.

References

- [1] (a) D.E. Webster, *Adv. Organomet. Chem.*, **15** (1977) 147; (b) A.E. Shilov and A.A. Shteinman, *Coord. Chem. Rev.*, **24** (1977) 97; (c) G.W. Parshall, *Homogeneous Catalysis*, Wiley-Interscience, New York, 1980; (d) R.H. Crabtree, in S. Patai and Z. Rappaport (eds.), *The Chemistry of Alkanes and Cycloalkanes*, Wiley, New York, 1992, p. 653.
- [2] (a) J.K. Hoyano and W.A. Graham, *J. Am. Chem. Soc.*, **104** (1982) 3723; (b) J.K. Hoyano, A.D. McMaster and W.A. Graham, *J. Am. Chem. Soc.*, **105** (1983) 7190.
- [3] (a) A.M. Janowicz and R.G. Bergman, *J. Am. Chem. Soc.*, **104** (1982) 352; (b) A.H. Janowicz and R.G. Bergman, *J. Am. Chem. Soc.*, **105** (1983) 3929; (c) R.A. Periana and R.G. Bergman, *Organometallics*, **3** (1984) 508; (d) M.J. Wax, J.M. Stryker, J.M. Buchanan, C.A. Kovac and R.G. Bergman, *J. Am. Chem. Soc.*, **106** (1984) 1211; (e) R.A. Periana and R.G. Bergman, *J. Am. Chem. Soc.*, **106** (1984) 7272.
- [4] (a) C.K. Ghosh and W.A. Graham, *J. Am. Chem. Soc.*, **109** (1987) 4726; (b) C.K. Ghosh, *Ph.D. Dissertation*, University of Alberta, Edmonton, Alberta, Canada, 1988.
- [5] (a) D.E. Marx and A.J. Lees, *Inorg. Chem.*, **27** (1988) 1121; (b) D.P. Drolet and A.J. Lees, *J. Am. Chem. Soc.*, **112** (1990) 5878; (c) D.P. Drolet and A.J. Lees, *J. Am. Chem. Soc.*, **114** (1992) 4186.
- [6] (a) S.T. Belt, D.M. Haddleton, R.N. Perutz, B.P.M. Smith and A.J. Dixon, *J. Chem. Soc., Chem. Commun.* (1987) 1347; (b) S.T. Belt, F.-W. Grevels, W.E. Koltzbücher, A. McCamley and R.N. Perutz, *J. Am. Chem. Soc.*, **111** (1989) 8373; (c) T.P. Dougherty and E.J. Heilweil, *J. Chem. Phys.*, **100** (1994) 4006; (d) W.T. Grubbs, T.P. Dougherty and E.J. Heilweil, *Chem. Phys. Lett.*, **227** (1994) 480.
- [7] (a) A.J. Rest, I. Whitwell, W.A.G. Graham, J.K. Hoyano and A.D. McMaster, *J. Chem. Soc., Chem. Commun.* (1984) 624; (b) A.J. Rest, I. Whitwell, W.A.G. Graham, J.K. Hoyano and A.D. McMaster, *J. Chem. Soc., Dalton Trans.* (1987) 1181; (c) P.E. Bloyce, A.J. Rest, I. Whitwell, W.A.G. Graham and R. Holmes-Smith, *J. Chem. Soc., Chem. Commun.* (1988) 846; (d) D.M. Haddleton, A. McCamley and R.N. Perutz, *J. Am. Chem. Soc.*, **110** (1988) 1810.
- [8] E.P. Wasserman, C.B. Moore and R.G. Bergman, *Science*, **255** (1992) 315.
- [9] (a) M.B. Sponsler, B.H. Weiller, P.O. Stoutland and R.G. Bergman, *J. Am. Chem. Soc.*, **111** (1989) 6841; (b) B.H. Weiller, E.P. Wasserman, R.G. Bergman, C.B. Moore and G.C. Pimentel, *J. Am. Chem. Soc.*, **111** (1989) 8288; (c) B.H. Weiller, E.P. Wasserman, C.B. Moore and R.G. Bergman, *J. Am. Chem. Soc.*, **115** (1993) 4326; (d) R.H. Schultz, A.A. Bengali, M.J. Tauber, B.H. Weiller, E.P. Wasserman, K.R. Kyle, C.B. Moore and R.G. Bergman, *J. Am. Chem. Soc.*, **116** (1994) 7369.
- [10] (a) A.J. Lees and A.A. Purwoko, *Coord. Chem. Rev.*, **132** (1994) 155; (b) A.A. Purwoko and A.J. Lees, *Inorg. Chem.*, **34** (1995) 424.
- [11] M.J. Schadt, N.J. Gresalfi and A.J. Lees, *Inorg. Chem.*, **24** (1985) 2492.
- [12] (a) E.O. Fischer and K. Bittler, *Z. Naturforsch. B*, **16** (1961) 225; (b) E.O. Fischer and K.S. Brenner, *Z. Naturforsch. B*, **17** (1962) 774; (c) J.W. Kang, K. Moseley and P.M. Maitlis, *J. Am. Chem. Soc.*, **91** (1969) 5970; (d) D.P. Drolet, *Ph.D. Dissertation*, SUNY-Binghamton, New York, 1991.
- [13] (a) C.A. Parker, *Proc. R. Soc. (Lond.) A*, **220** (1953) 104; (b) C.G. Hatchard and C.A. Parker, *Proc. R. Soc. (Lond.) A*, **235** (1956) 518; (c) J.G. Calvert and J.N. Pitts, *Photochemistry*, Wiley, New York, 1966; (d) H.G. Heller and J.N. Langan, *J. Chem. Soc., Perkin Trans.* (1981) 341.
- [14] G.L. Geoffroy and M.S. Wrighton, *Organometallic Photochemistry*, Academic Press, 1979.
- [15] (a) D.M. Manuta and A.J. Lees, *Inorg. Chem.*, **22** (1983) 3825; (b) D.M. Manuta and A.J. Lees, *Inorg. Chem.*, **25** (1986) 3212; (c) M.M. Glezen and A.J. Lees, *J. Am. Chem. Soc.*, **111** (1989) 6602.
- [16] M.S. Wrighton, H.B. Abrahamson and D.L. Morse, *J. Am. Chem. Soc.*, **98** (1976) 4105.
- [17] (a) M. Saito, J. Fujita and K. Saito, *Bull. Chem. Soc. Jpn.*, **41** (1968) 359; (b) M.S. Wrighton and D.L. Morse, *J. Organomet. Chem.*, **127** (1975) 405; (c) H.B. Abrahamson and M.S. Wrighton, *Inorg. Chem.*, **17** (1978) 3385.
- [18] A.J. Lees, *Chem. Rev.*, **87** (1987) 711.
- [19] P.E. Bloyce, J. Mascetti and A.J. Rest, *J. Organomet. Chem.*, **444** (1993) 223.